Monodisperse nanocrystals: general synthesis, assembly, and their applications

Xun Wang and Yadong Li*

Received (in Cambridge, UK) 8th January 2007, Accepted 2nd February 2007
First published as an Advance Article on the web 28th February 2007
DOI: 10.1039/b700183e

This article summarizes the recent advances in the synthesis, assembly and applications of monodisperse nanocrystals, which may be suggestive for the designed synthesis and assemblies of target nanocrystals according to practical requirements.

Introduction

Over the past decade monodisperse nanocrystals, which exhibit many interesting shape- and size-dependent phenomena and properties, have been extensively investigated for both their scientific and technological applications.[1–4] With the growing interest in building advanced materials using these novel building blocks,[5–15] the development of a facile synthetic method towards such high quality nanocrystals with uniform size and shape appears to be of key importance for the exploration of new research and application fields, and various synthetic approaches such as organometallic and organic-solvent-based synthetic routes *etc*, have been established.[3,16,17] To realize their applications in macroscopic scale, assembly of discrete nano-building blocks into controllable architectures and materials with advanced functions is also of increasing importance in chemistry and materials science,[18] and by utilizing noncovalent interactions self-assembly and self-organization provide feasible tools to generate advanced and functional nanometre and micrometre superstructures from various nano-objects.[5,19–21] Meanwhile, based on the nanocrystals or nanocrystal assemblies, many new and promising fields have been explored, including biological labeling,[22,23] catalysis[24,25] and sensor fields,[26,27] *etc*. All these make the whole research field of monodisperse nanocrystals.

Department of Chemistry, Tsinghua University, Beijing, 100084, P. R. China. E-mail: ydli@tsinghua.edu.cn; Fax: 8610 62788765; Tel: 8610-62772350

The controlled growth, assembly and applications of monodisperse nanocrystals are typical interdisciplinary fields, which involve numerous chemical and physical contents. Although each of these research fields deserves special research attention, a general understanding on the whole picture of these fields may give us more inspiration: for example, monodisperse nanocrystals have shown size and shape dependent catalytic properties for structure-sensitive reactions, which may serve as the basis for the design of new types of nanocatalyst; for the potential applications in catalysis, a much closer look at the catalytic process may help us to choose appropriate experimental conditions to realize the controlled growth of these nanocrystals so that they exhibit the best catalytic performance. It is useful to pave the way to the practical applications of these novel nanocrystals when developing new synthetic strategies and assembly methods. As a feedback, the practical applications of these novel nanocrystals will make further demands on synthetic strategies towards more precise control over surface properties, size and dimensionalities. To design the chemical and physical properties of the target nanocrystals or nanocrystal assemblies according to practical requirements is a further important issue in this field.

This article summarizes our recent endeavors on the synthesis, assembly and applications of monodispere nanocrystals. Based on solvothermal methods and interface-mediated reactions, general synthetic methods have been developed to obtain various monodisperse nanocrystals; *via* noncovalent interactions, self-assembly of nanocrystals into

Xun Wang

Xun Wang received his BS degree in Department of Chemical Engineering, Northwest University (China) in 1998, and his PhD degree in Department of Chemistry, Tsinghua University in 2004, with Yadong Li. He joined the faculty of Department of Chemistry, Tsinghua University in 2004, and became an associate professor in 2005.

Yadong Li

Yadong Li received his BS degree in Department of Chemistry, Anhui Normal University in 1986 and his PhD degree in Department of Chemistry, University of Science and Technology of China in 1998, with Yitai Qian. He joined the faculty of Department of Chemistry, Tsinghua University in 1999 as a full professor.

two-dimensional arrays is achieved; then as an illustration of the possible applications of the as-obtained nanocrystals, shape-dependent catalytic properties and their use as biosensors have been demonstrated, which may be suggestive for the exploration of this new, interesting and promising field.

Solvothermal synthesis of monodisperse nanocrystals

Solvothermal synthesis utilizes a solvent under elevated pressures and temperatures (above or below its critical point) to increase the solubility of a solid and to speed up reactions between solids. The goal in using solvothermal reactions is to precipitate new solids from the reaction medium, which may have crystalline structures different from the thermodynamically stable phases formed under normal high-temperature synthesis conditions.[28,29] The solvothermal process has recently been extensively applied to the synthesis and design of monodisperse nanocrystals with new structures and properties because suitable solvents/stabilizing agents can modulate the growth dynamics of the nanocrystals and prevent the particles from undergoing agglomeration.[30–36]

This solvothermal method can be regarded as a modification of traditional organic-solvent-based routes, which have been the most common way to obtain monodisperse nanocrystals ever since the organometallic approach was introduced in the early 1990s.[16] The difference in the above two strategies is that the solvothermal process proceeds in a sealed vessel, the temperature and pressure of which can be designed with no limitation provided they are safe for the vessel, while the temperature of the traditional organic-solvent-based routes is limited by the boiling point of the solvents. This important feature makes the solvothermal method very flexible in designing the reaction system.

A typical synthesis system for the solvothermal method consists of three components: precursors, organic surfactants and solvents. The precursors can be organometallic compounds, metal complexes or inorganic species, and the temperature can be controlled below or above the boiling point of the solvents, depending on the solvents/surfactants system. Undoubtedly, the choice of solvents, surfactants and the precursors are the key to the success of this approach.

Fatty acids such as oleic acid and linoleic acid have been proved as good solvents and surfactants for the growth of nanocrystals under solvothermal conditions. By controlling the hydrolysis reaction of $Ti(OBu)_4$ using NH_4HCO_3 and linoleic acid (LA), highly crystalline, near monodisperse and redispersible TiO_2 nanorods (Fig. 1(a)) and nanoparticles (Fig. 1(b)) and their metal-ion-doped derivatives (*e.g.* Sn^{4+}, Fe^{3+}, Co^{2+} (Fig. 1(c), Ni^{2+}, *etc.*), have been synthesized.[30] Linoleic acid and cyclohexane were adopted as co-solvents while the linoleic acid also acted as a protecting reagent (surfactant) for TiO_2 nanocrystals. Because the solvent cyclohexane has a very low boiling point (about 80 °C), the reflux temperature was not high enough to achieve crystalline products with conventional solution reflux conditions. Control experiments were carried out using a conventional open solution reflux system, but neither nanorods nor nanoparticles were obtained. Thus the solvothermal method was chosen to obtain highly crystalline TiO_2 at low temperatures. The solvothermal reactions were carried out in a sealed autoclave in what could be considered to be an isochoric-closed system, which could provide suitable conditions for the hydrolysis, polycondensation reactions, and the final formation of nanorods and nanoparticles. In the solvothermal system (the volume of the system does not change), the reaction temperature could be 150 °C or more, much higher than the boiling point of cyclohexane. Thus, the reactivity of the reactants might be improved and crystalline TiO_2 nanorods (without the addition of NH_4HCO_3) could be obtained. The sealed system prevented the volatilization of the gases (H_2O, CO_2 and NH_3), thus the addition of NH_4HCO_3 can modulate the growth dynamics of the TiO_2 nanocrystals. With the decomposition of NH_4HCO_3, H_2O can be kept inside the system to react with $Ti(OBu)_4$ to form the nanoparticles. The chain length of carboxylic acids also had great influence on the formation of TiO_2. Different types of carboxylic acids such as decanoic acid ($C_9H_{19}COOH$), valeric acid (C_4H_9COOH), acetic acid (CH_3COOH), and so forth have been used as solvents and surfactants. TiO_2 nanoparticles and nanorods were obtained by using decanoic acid; however with valeric acid and acetic acid, TiO_2 deposition did not occur. Based on these experimental facts, it was believed that long-chain organic acids are important and necessary in the formation of TiO_2.

This cyclohexane (hexane)–fatty acid–based solvothermal system can be further applied to the synthesis of monodisperse

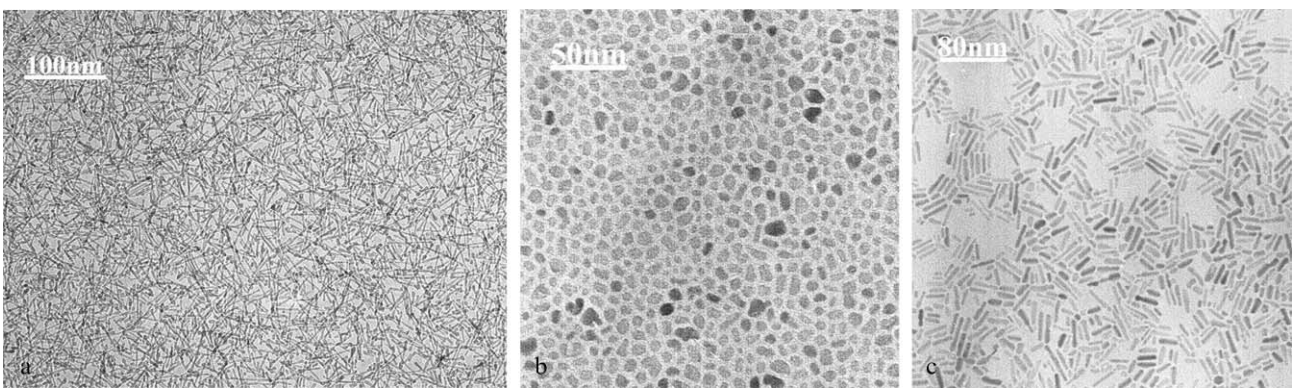

Fig. 1 TEM images of TiO_2 nanocrystals obtained from solvothermal method; (a) TiO_2 nanorods, (b) TiO_2 nanoparticles; (c) TiO_2 nanorods doped with Co^{2+}.

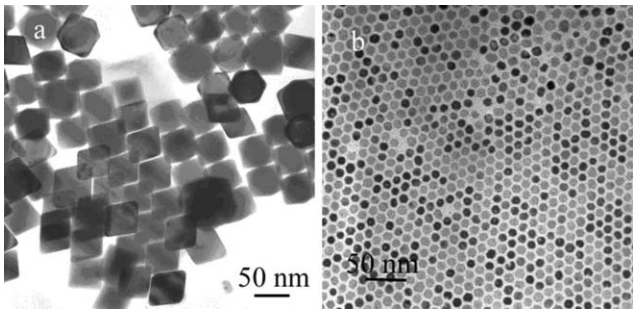

Fig. 2 TEM images of PbSe nanocrystals: 50 nm polyhedral (a) and 12 nm round (b).

Fe_3O_4[32] or ZnS[33,34] nanocrystals with inorganic salts such as $FeCl_3$ and $ZnCl_2$ as precursors. Besides long alkyl chain fatty acids, long-chain amines such as octadecylamine was also used as solvents and protecting reagents to synthesize II–VI semiconductor nanocrystals such as PbSe.[35] The sizes and shape of the nanocrystals varied with parameters such as reaction time, temperature and molar ratio of reactants (Fig. 2). Since the complex reaction between the fatty acid/amine and metal ions are quite general, it is believed that these model systems can be further expanded to the synthesis of many other oxide or non-oxide nanocrystals.

Covered with long alkyl chain fatty acids or amines, the as-obtained nanocrystals from fatty acid/amine solvothermal systems usually have hydrophobic surface properties, and this greatly inhibits their applications in areas such as biotechnology and biomedicine. In order to obtain monodisperse nanocrystals with hydrophilic properties, ethylene glycol has been adopted as solvent in the solvothermal synthesis of magnetic ferrite nanocrystals (Fig. 3) with polyethylene glycol or hexanediamine as protecting reagents.[31,36]

Based on the experimental facts, it is believed that ethylene glycol plays an important role in the formation of the ferrites. Ethylene glycol has been widely used in the polyol process for providing monodisperse fine metal or metal oxide nanoparticles.[4] However, magnetic spinel ferrite particles have a strong tendency to agglomerate during their formation in such a liquid-phase process. In order to obtain monodisperse Fe_3O_4 particles, a modified synthetic route was designed, in which two additives were found as critical elements in the system. First, sodium acetate (NaAc) was added for electrostatic stabilization to avoid particle agglomeration. In this system, the addition of NaAc also seemed to help ethylene glycol reduce $FeCl_3$ to Fe_3O_4. Control experiments showed that Fe^{3+} could not be reduced by ethylene glycol alone in the same reaction conditions. Secondly, poly(ethylene glycol) was added as surfactant in the system to prevent particle agglomeration. Series of magnetic ferrite microspheres or hollow spheres have been obtained based on this polyol solvothermal method.

By carefully choosing solvents and protecting reagents, different types of monodisperse nanocrystals with hydrophobic or hydrophilic properties can be readily prepared. It is worthy to note that, besides the above-mentioned nanostructures, solvothermal synthesis might have great potential in the controlled synthesis of monodisperse nanostructures of metastable oxide or non-oxide compounds, one of the main advantages of this novel strategy.

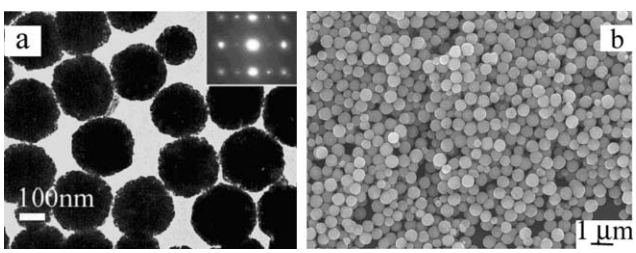

Fig. 3 (a) A typical TEM image of $MnFe_2O_4$ microspheres with diameter ~200 nm; the inset shows the electron diffraction pattern. (b) SEM image of $MnFe_2O_4$ microspheres with diameter ~800 nm.

General synthesis of monodisperse nanocrystals *via* interface-mediated approaches

Although the above-mentioned solvothermal method and the traditional organic-solvent-based synthetic routes can be used to prepare various monodisperse nanostructures, the success of these strategies greatly depend on the exploration of new reaction systems for specific target nanostructures. Due to the diverse crystal structures and physical/chemical properties of different compounds, it is still a hard challenge to develop a general synthetic strategy for nanocrystals, which may be the key in the understanding of the controlled growth of low-dimensional nanostructures and may bring some more opportunities to nano-related fields.

As a general synthetic procedure, one requires precursors in general forms and the reactions taking place under similar experimental conditions, which would be impossible for solvothermal and organic-solvent-based routes requiring careful choice of precursors and solvents. Interface-controlled strategies have been developed to partly meet this challenge, which are described as liquid–solid–solution phase transfer and separation strategy (Fig. 4)[37] and water/oil interface-controlled reaction in normal emulsions (Fig. 5),[38] respectively. In these approaches, a water–ethanol mixed solution is

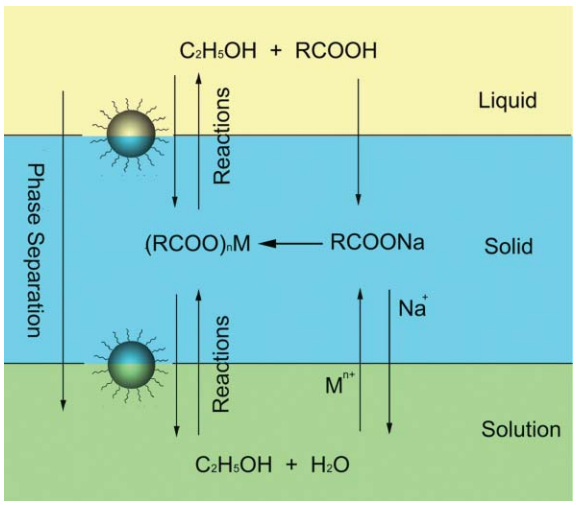

Fig. 4 Scheme of liquid–solid–solution (LSS) phase transfer and separation synthetic strategy.

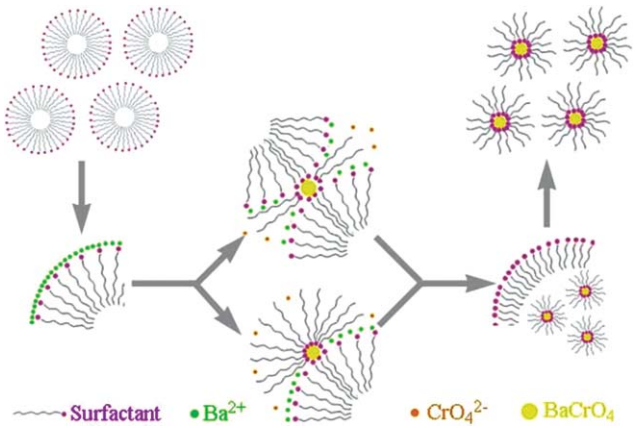

Fig. 5 Proposed mechanism for the synthesis of colloidal nanoparticles *via* oil/water interface-controlled reaction in normal microemulsions.

adopted as the main continuous solution phase. Since water is an ideal solvent for most inorganic species, and ethanol is good solvent for most of the surfactants including fatty acids, most soluble inorganic salts can be adopted as the starting materials and long alkyl chain surfactants such as octadecylamine or oleic acid can be used as protecting reagents for the nanocrystals; fatty acid/amines as ordinary complexation reagents have been widely adopted as the protecting reagents for nanocrystals, and more importantly they can complex with different meal ions to form metal salts, which may covalently combine the surface of the nanocrystals and prevent agglomeration; so fatty acid/amine as both precursors and protecting reagents are good choices for the developing of a general synthetic method, and in these approaches linoleic acid and sodium linoleate (or amine) have been adopted. Along with the reactions and the ion exchange process of sodium linoleate and the metal ions across the different phases, linoleic acid can be released during the reactions, and the *in-situ* generated nanocrystals will be covered with the long alkyl chains and thus have hydrophobic surfaces, which is incompatible with the hydrophilic surrounding of the aqueous solution. As a result, these hydrophobic nanocrystals will be separated from the bulk aqueous solution spontaneously (in case of LSS strategy) or by the addition of ethanol (in the case of water/oil interface-controlled reaction in normal emulsions) and then collected at the bottom of the vessel. Since they are covered with long alkyl chains, these nanocrystals usually have hydrophobic surface properties, and can be redispersed into nonpolar solvents such as cyclohexane and chloroform.

By carefully designing the chemical reactions that occur at the interfaces of different phases or at the water/oil interfaces, a huge group of monodisperse nanocrystals with sizes in the range of 2–15 nm, which have quite different crystal structures, compositions and properties have been obtained, including noble metals (Fig. 6(a); Ag, Au, Pd, Pt, Ru, Rh, Ir), magnetic/dielectric[39] (Fe_3O_4, $CoFe_2O_4$, $MnFe_2O_4$, $ZnFe_2O_4$, $BaTiO_3$, $SrTiO_3$, *etc.*), semiconductors[40–42] (Fig. 6(b); PbS, Ag_2S, CdS, ZnS, ZnSe, CdSe, TiO_2, ZrO_2, CuO), rare earth fluorescent[43–46] ($NaYF_4$, YF_3, LnF_3, $Ln(OH)_3$), biomedical[47] ($Ca_{10}(PO_4)_6(OH)_2$, $CaCO_3$), and other monodisperse organic optoelectronic semiconductors (Metal Phthalocyanine), and conducting polymers (PPy and PAn) nanoparticles *etc*.

Besides uniform nearly round-shaped nanocrystals, these interface-mediated approaches have shown their potential in controlling the shape of the as-obtained nanocrystals. For example, by altering the temperature or concentration conditions, apatite nanorods with different lengths have been obtained.[47] Also by controlling the doping concentration of Ln^{3+} ions or Y^{3+}/F^- ratio, the shape and size of luminescent $NaYF_4$ can be rationally controlled.[44,46]

For the potential biological application of monodisperse hydrophobic nanoparticles, it is necessary to modify the surface to make these particles water-soluble and biocompatible.[22,23] The silica-coating method was selected for polarity transformation because silica surfaces are biocompatible and can be easily functionalized for bioconjugation purposes. A silica shell was coated around the nanocrystals (for example, CdSe, ZnSe,[41] $NaYF_4$[48] nanoparticles) *via* a water-in-oil

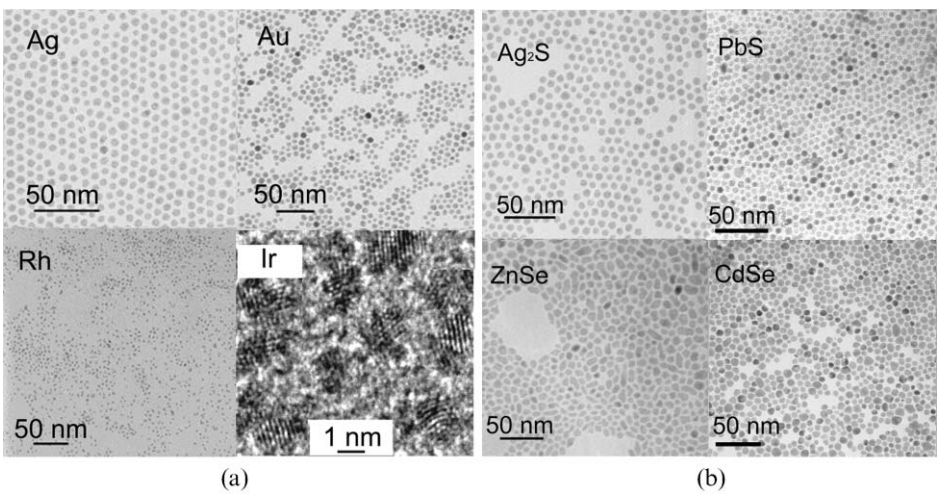

Fig. 6 (a) TEM images of Ag (6.1 ± 0.3 nm), Au (7.1 ± 0.5 nm), Rh (2.2 ± 0.1 nm) and Ir (1.7 ± 0.09 nm) nanocrystals synthesized *via* LSS strategy. (b) TEM images of semiconductor nanocrystals; Ag_2S (7.3 ± 0.4 nm), PbS (5.7 ± 0.2 nm), ZnSe (8.2 ± 0.9 nm), CdSe (7.1 ± 0.8 nm) *via* LSS strategy.

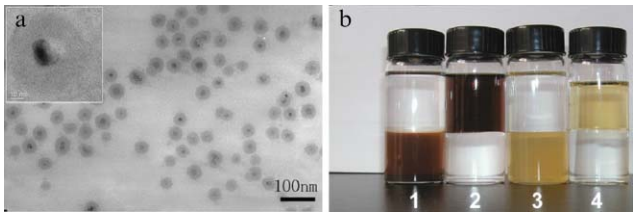

Fig. 7 (a) TEM image of silica-sheathed ZnSe nanocrystals. The inset is an HRTEM image of a single particle. (b) The upper layer is *n*-hexane and the bottom layer is deionized water. From left to right, the bottles contain $CdSe/SiO_2$ in water, CdSe in hexane, $ZnSe/SiO_2$ in water, and ZnSe in hexane.

microemulsion method in reference to the classic Stober method. As shown in Fig. 7, the size of the $ZnSe/SiO_2$ core structure was about 40 nm, and they could be well dispersed in alcohols and water (Fig. 7(a) and (b)). After the particles were coated with silica, the electronic absorption spectra were also measured, and they suggested that the conversion does not change the intrinsic properties of these semiconductor particles. Further endeavors on the surface modification and bioapplication of the as-prepared nanocrystals are under way.

It is apparent that the current LSS and oil/water interface-controlled reaction strategies are superior to the reported synthetic methods in general, which provide us with a general understanding on the formation mechanism concerning the interface-mediated growth. More studies are still needed to improve these strategies in precise control over shape, size and the surface properties of the nanocrystals.

Assembly *via* the interaction of surfactants absorbed on the surfaces of nanocrystals

In nanosystems, self-assembly offers one of the few practical strategies for assembling components into larger, functional ensembles through different interactions.[18] As ''artificial atoms'', uniform nanocrystals receive increasing attention and extensive investigation, and these nanostructures will be promising building blocks for advanced materials and bottom-up approaches to the fabrication of nanodevices.

A self-assembly strategy has been developed to obtain the two-dimensional superstructures of uniform nanocrystals with different chemistries and properties.[20,21] The as-prepared nanocrystals, with long-chain alkyl molecules attached to the crystal surface, could be patterned by noncovalent interactions in a natural and spontaneous process occurring mainly through noncovalent interactions such as van der Waals, hydrogen bonding, hydrophilic/hydrophobic, electrostatic and metal–ligand coordination networks.[5,49] Considering the intrinsic nature of supramolecular chemistry and common characteristics of the synthesis process, it is believed there are two key factors to direct the self assembly of functional nanocrystals (NCs) into higher-order superstructures: specific shapes and long-chain alkyl modified surfaces. The shape effect is of particular importance due to their original nature in assembly while the interactions between the long-chain alkyls on the crystal surface would induce the crystal to assemble into certain patterns (Fig. 8).

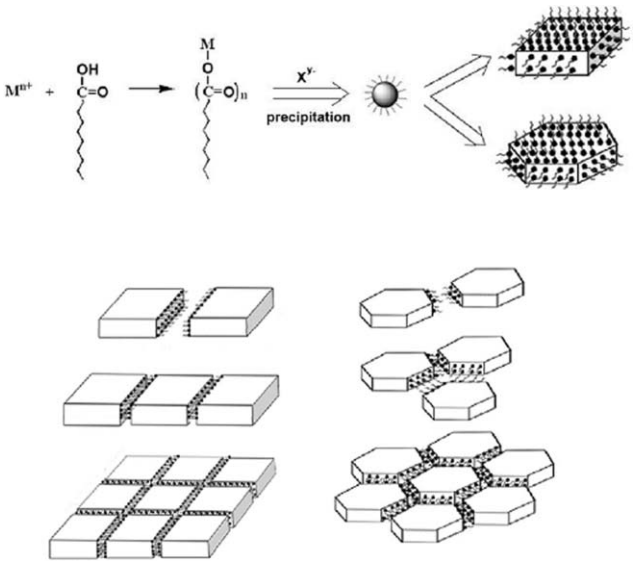

Fig. 8 Proposed schematic illustration of assembly of NCs.

Taking hexagonal nanocrystals as an example, a corresponding HRTEM image (Fig. 9), taken from the edge of the nanocrystals, showed that the crystallized core was surrounded by an obviously uncrystallized overlayer. The thickness of the uncrystallized overlayer was 1.7 ± 0.1 nm, nearly consistent with a monolayer of an oleic acid (OA) molecule. More information from the surface was obtained by FT-IR analysis, Raman spectroscopy and electron energy loss spectroscopy (EELS).[20] Clearly, the characteristic results revealed the uncrystallized overlayer was formed by close-packed OA molecules on the surface of the nanocrystals. The length of OA molecule is *ca.* 2 nm, so the absorbed OA molecule might tilt at a certain angle. Moreover the sharpness of the bands at 2927 cm^{-1} ($\nu_{as}(CH_2)$) and 2856 cm^{-1} ($\nu_s(CH_2)$) in the FT-IR

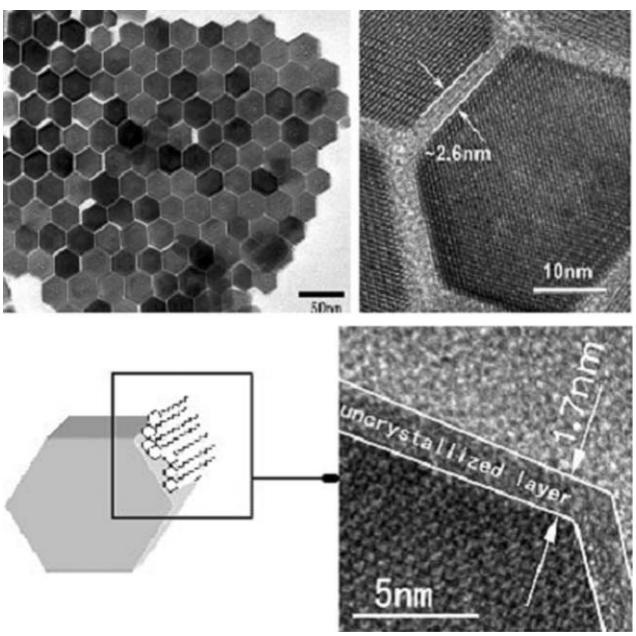

Fig. 9 TEM images of yttrium phosphate hydrate NCs and HRTEM image on the edge of an yttrium phosphate hydrate.

spectrum indicates the hydrocarbon chains were well ordered. In the HRTEM image (Fig. 9), it can be evidenced that the assembled H-nanocrystals were separated by an interparticle spacing of (2.6 $\pm$ 0.2 nm). Since the spacing was smaller than the double thickness of OA monolayer (1.7 nm), this indicated that either a considerable overlap of aliphatic tails or a certain tilt angle might be present. The first case, the OA molecules interdigitating each other to form an ''arm to arm'' interaction, is more favorable to the assembly of complex structures. The interparticle spacing (2.6 $\pm$ 0.2 nm) was nearly 1.5 times the size of OA monolayer (1.7 nm), indicating that half the alkyl chain of the OA molecules (nearly 9 C atoms) interdigitated. Furthermore, molecular mechanics calculations proved that the interdigitating of OA would efficiently minimize the energy of system. Both the manner and degree of overlap enormously affected the stability of the superstructures. Compared with hexagonal (H) nanocrystals, tetragonal (T) nanocrystals were separated by smaller interspacing, indicating that more overlap of OA occurred (Fig. 10). Namely, to form stable complex superstructures of T-nanocrystals stronger interaction was necessary due to the shape effect.

These results revealed that several proposed factors contributed to the success of self-assembly in this process. First, the uniform assembled superstructures were more stable than the dissociated nanocrystals or disordered aggregates. Second, hydrophobic OA would facilitate the self-assembly process over long distances resulting from minimization of the interfacial free energy. Particularly, hexagonal nanocrystals can self-assemble into more regular superstructures due to the shape effects. Hexagons with higher symmetry can utilize minimum material to occupy maximum area and spontaneously assemble to close-packed superstructures. On the other hand, in this case, if assembled patterns contain some defects, other hexagonal nanocrystals or pieces will move easily into the patterns and improve the structure after a little adjustment. However, tetragonal or other more irregular nanocrystals were only packed in the direction that led to a larger contact surface, and cannot pack as easily as hexagonal nanocrystals.

By adopting the same strategy, we have also successfully assembled PbSe with uniform polyhedral shape to a 2D pattern by utilizing the interaction of long-chain octadecylamine. The results also indicated that half the alkyl chain of the octadecylamine molecules interdigitate and further confirmed our supposition.

The strategy based on interaction of long-chain alkyls and uniformity of nanocrystals provides us with the ability to fabricate functional close-packed superstructures of nanocrystals as ''artificial solids'' by self-assembly. The experimental results show the direct proof that interaction of OA (or other long-chain alkyl molecules) contributes to successful assemblies to different degrees. Meanwhile we also demonstrate that shape effects play an important role in the assembly process. More uniformity of nanocrystals will bring more spontaneity and order in assembly. The promising strategy opens an avenue to manipulating the ''artificial atoms'' to form 2-D or 3-D ''artificial solids'', namely, even to build advanced nanodevices in the future.

Applications of monodisperse nanocrystals

Shape and size are the main factors that determine the chemical and physical properties of monodisperse nanocrystals, which may serve as bases for the development of new industry fields. Based on the size effect of quantum dots such as CdSe, biological labeling system have been developed to realize detection of biological species.[22,23] Magnetic nanocrystals with uniform sizes and specific shape have shown potential

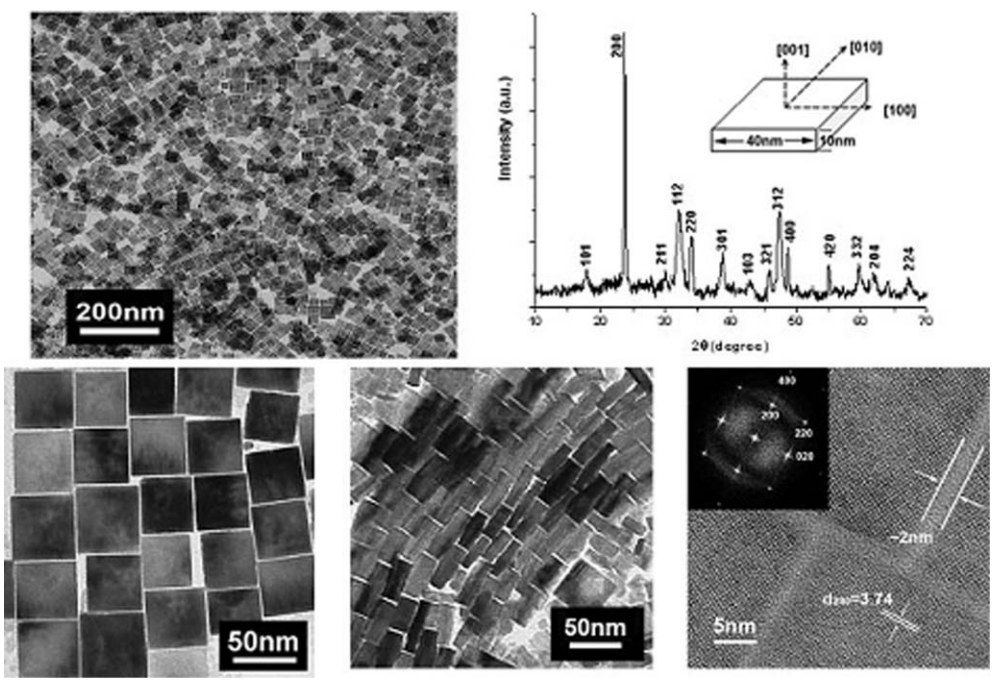

Fig. 10 TEM and HRTEM images of lanthanum vanadate nanocrystals.

in high-density data storage[50] and magnetic bio-separation fields.[51] As for the shape effect, the SERS effects of metal nanocrystals with different shape and dimensionality are being currently investigated.[52,53] With the development of general synthetic strategies, more functional nanocrystals with controlled size and shape can be readily obtained, which deserve more attention for their potential in both research and applications.

Shape-dependent catalytic performance of nanocrystals

Nanostructured materials present great promise and opportunities for a new generation of catalysts. Catalysts are mostly nanoscale particles, and catalysis is a nanoscale phenomena.[54] It is known that the reactivity depends on the crystal plane of the catalyst for structure-sensitive reactions.[55] A typical case may be iron catalysts used for the synthesis of ammonia. It was observed that preferentially exposed {111} planes at the surface of iron were crucial to generating excellent activity.[56] Recently, Choudary *et al.* reported that MgO hexagonal crystals exposing the most {100} planes were more active than nanocrystalline samples.[57] Therefore, a desirable goal for catalyst design and synthesis would be to decrease the area of the less reactive crystal planes and increase that of the more reactive ones so as to optimize the desired structure of the active sites. Although large single-crystal model catalysts are characteristic of these features, the surface area of the "effective" planes is very small and far from practical application. Shape-controlled synthesis of nanostructured materials may present an opportunity for the synthesis of catalytic materials with such desirable features because these novel materials nucleate and grow in an epitaxial manner, exposing defined crystal planes.

CeO_2 nanorods and nanoparticles have been synthesized *via* a hydrothermal method and a direct precipitation method, respectively.[25] Cross-sectional views indicated that the as-prepared CeO_2 nanorods were single crystalline and the preferential growth direction was [110] (Fig. 11). An HRTEM image of the CeO_2 nanoparticles (Fig. 12) showed that the dominant lattice fringes were from {111}, which were observed when the particles were oriented along the [110] direction. The particles showed two types of shapes: one was octahedral, enclosed by eight {111} planes, and the other truncated octahedral, enclosed by eight {111} and six {001} planes. Obviously, the predominantly exposed planes were the {111} in the CeO_2 nanoparticles, with a small amount of {001} planes. Measurements were made of the catalytic activity of CO oxidation. It was clear that CeO_2 nanorods were more active than CeO_2 nanoparticles. At 190 °C, the percentage CO conversion was 40% over the CeO_2 nanorods and only 17% over the nanoparticles (Fig. 13). The rate of conversion over CeO_2 nanorods was three times higher than that over nanoparticles. In general, high-surface-area nanocatalytic materials exhibiting numerous crystal faces, edges, and corners, which are conventionally considered active sites for the adsorption of reactants,[58] should generate better catalytic performance. However, in the present study CeO_2 nanoparticles, with higher surface area and smaller particle size, were poorer catalysts, whereas CeO_2 nanorods, with lower surface

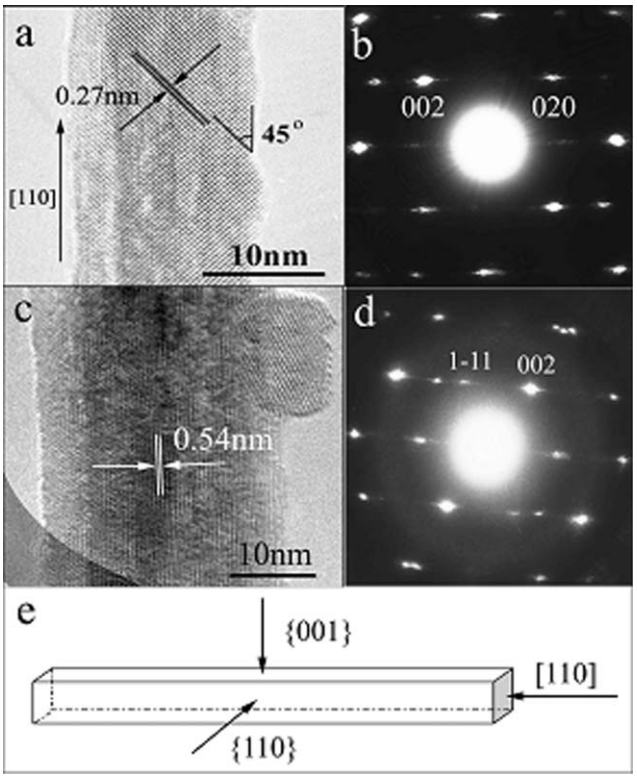

Fig. 11 (a) Magnified HRTEM of a typical nanorod view along [001]; (b) the SAED pattern of (a); (c) magnified HRTEM of a typical nanorod view along [110]; (d) the SAED pattern of (c); (e) the structural models of CeO_2 nanorods.

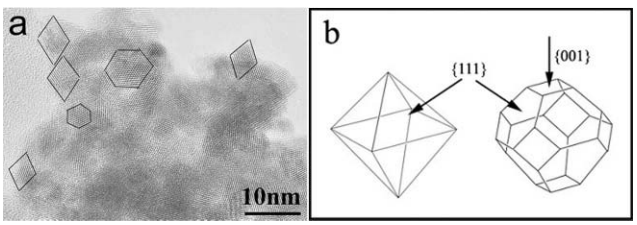

Fig. 12 (a) HRTEM image of the CeO_2 nanoparticles; (b) structural models of the octahedral and truncated octahedral shapes of CeO_2 nanoparticles.

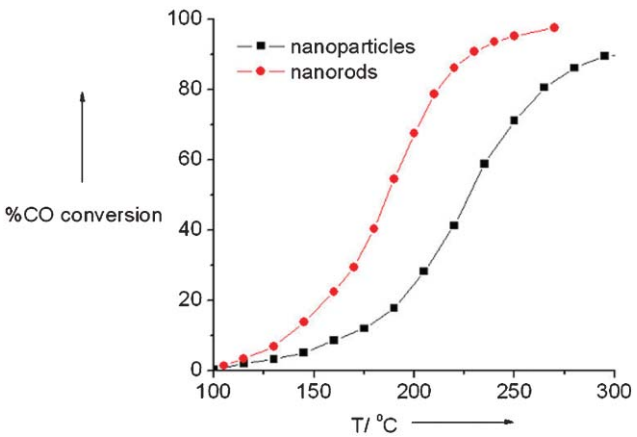

Fig. 13 Percentage conversion *vs.* temperature plots for the oxidation of CO over (a) CeO_2 nanoparticles and (b) CeO_2 nanorods.

area and larger diameter, were more active and demonstrated a stable redox property. These unusual results for these two ceria nanomaterials inspire us to hope that specific crystal planes are indeed a determining factor that will prove useful.

Similar phenomena were observed in the study on the catalytic performance of CuO[59] and Ag[60] nanocrystals with different shapes. The CuO nanocrystallites with different shapes and different surface orientations could be synthesized by controlling a few critical synthesis parameters. It was found that the reducibility and catalytic reactivity of the CuO nanostructures depended on the shape and the exposed crystal planes. The CuO nanoplatelets exposing the $(01\bar{1})$ planes released oxygen from the surface lattice more easily, followed by the nanobelts with (001) planes; in turn they were more active than the nanoparticles with close-packed (111) planes. Subsequent investigation was carried out in silver nanocrystal systems. Truncated triangular silver nanoplates with well-defined planes were synthesized by a simple solvothermal approach. The activity of these truncated triangular silver nanoparticles was compared with that of cubic and near-spherical silver nanoparticles in the oxidation of styrene in colloidal solution. It was found that the crystal faces of silver nanoparticles played an essential role in determining the catalytic oxidation properties. The silver nanocubes had the {100} crystal faces as the basal plane, whereas truncated triangular nanoplates and near-spherical nanoparticles predominantly exposed the most-stable {111} crystal faces. As a result, the rate of the reaction over the nanocubes was more than 14 times higher than that on nanoplates and four times higher than that on near-spherical nanoparticles.

The present results indicate that the recent development of shape-controlled synthesis of nanocrystals may be helpful for designing novel catalysts with desired performance.[59–61] With the further development of synthetic strategies, monodisperse nanocrystals with precisely controlled shape and size would be obtained in a much easier way, so that catalysts may be ''designed'' rather than ''prepared''.

Upconversion rare-earth nanocrystals as biosensors

The rapid development of diagnostics of infectious and genetic diseases, and methodologies for forensic and genetic identification is now challenging chemists to find more efficient biological labels than traditional organic dyes. These labels should be resistant to photobleaching, nontoxic, biocompatible, monochromatic, highly luminescent, and, more importantly, ultrasensitive in both *in vitro* and *in vivo* bioassays. Various semiconductor quantum dots (QDs) with tunable size-dependent emission, high quantum yields of photoluminescence (PL), broad excitation spectra, and narrow emission bandwidths have been developed and successfully applied in biological analyses.[22,23] However, their inherent toxicity and chemical instability limits their application in biological detection and medical diagnosis. On the other hand, although these QDs work well under laboratory conditions, an increase in their background signal may be noted in the presence of interfering biomolecules (such as green fluorescent proteins) and other fluorescent organic molecules that are usually present in biological and environmental samples, which can also be excited by UV radiation. Hence, to find a more appropriate luminescent label remains a challenging task.

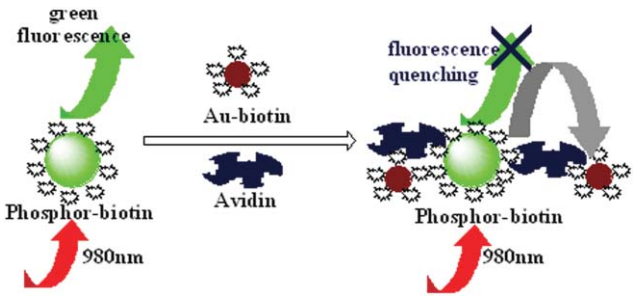

Fig. 14 Scheme of the FRET system, with phosphor-biotin nanoparticles as energy donors and Au-biotin nanoparticles as energy acceptors, in the analysis of avidin. ET = energy transfer.

Upconversion (UC) nanophosphors, which are excited in the IR region instead of the UV region to give emission in the visible domain, may be such an alternative. These UC nanophosphors show a high chemical stability, high quantum yields, and low toxicity, and their optical properties can be tuned by variation of lanthanide dopants and the host matrix.[62] In particular, the fluorescence from biological samples (background) upon excitation with IR radiation is extremely low as the interfering biomolecules in question absorb in the UV (not the IR) region. All these favorable properties indicate the great potential of UC nanoparticles in the analysis of biological and environmental samples, and especially for fluorescence imaging *in vivo*.[63]

A novel biosensor for the detection of trace amounts of avidin was designed, which was based on fluorescence resonant energy transfer (FRET) between bioconjugated UC nanoparticles and gold nanoparticles (Fig. 14). The UC nanoparticles we chose were $Na(Y_{1.5}Na_{0.5})F_6:Yb^{3+},Er^{3+}$. The nanoparticles showed three emission bands at λ = 525, 540 and 655 nm, which correspond to energy-transfer processes from the excited states $^2H_{11/2}$, $^4S_{3/2}$, and $^4F_{9/2}$, respectively, to the ground state $^4I_{15/2}$ (Fig. 15). However, the peak at 540 nm was the main

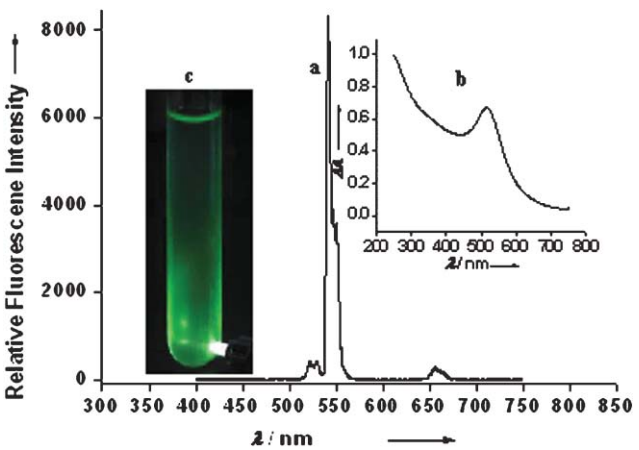

Fig. 15 (a) Upconversion luminescence spectrum of hexagonal-phase upconversion nanoparticles in solution upon excitation with a 980 nm laser; (b) green luminescence observed from sample. (c) UV/Vis absorption spectrum of 7-nm gold nanoparticles in aqueous solution.

peak, while the other peaks were very weak in comparison. As typical organic fluorescent dyes displayed broad emission spectra with a long tail, an ''impurity'' in the form of the emission from the nanoparticles could introduce spectral cross-talk between different detection channels which thus make them unsuitable for biological applications and creates difficulties in the quantification of the relative amounts of different probes. Here, the monodispersed nanoparticles emitted strong and pure green fluorescence with a symmetric and narrow emission spectrum upon excitation at a single wavelength (980 nm laser), which made them more suitable as a probe for multicolor biological detection. It is also well-known that gold nanoparticles have good absorption properties in the UV region. The 7-nm gold nanoparticles used in our experiments showed a strong absorption at 520 nm (Fig. 15), which matched well with the UC emission of $Na(Y_{1.5}Na_{0.5})F_6:Yb^{3+},Er^{3+}$. According to the theory of FRET, when the absorption of the energy acceptor is close to the emission of the phosphor and when the donor and the acceptor are close enough, the emission of the energy donor (upconversion phosphor nanoparticles) would be quenched by the energy acceptor (gold nanoparticles). Thus it is intrinsically possible to couple the UC $Na(Y_{1.5}Na_{0.5})F_6:Yb^{3+},Er^{3+}$ nanoparticles (energy donors) with 7-nm gold nanoparticles (energy acceptors) to give a FRET biosensor.

To test the UC phosphor-based FRET biosensor, first, UC and gold nanoparticles were functionalized by the layer-by-layer (LbL) method[64] to introduce an NH_2 group that could be attached to biotin (Fig. 16). Then different concentrations of avidin were added to the mixture of the biotin-phosphor nanoparticles (80 nm) and Au-biotin nanoparticles (144 nm), and PL spectra were measured as a function of the concentration of avidin. When avidin was added, Au-biotin nanoparticles were conjugated to the surface of the UC phosphor-biotin nanoparticles through the sensitive and selective interaction between avidin and biotin. As shown in Fig. 17, the luminescence was gradually quenched with increasing amounts of avidin added to the system. Fig. 17

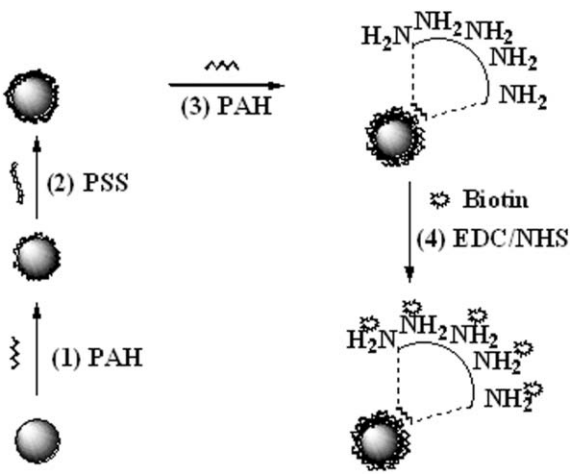

Fig. 16 Schematic illustration of the functionalization of the upconversion nanoparticles. PAH = poly(allylamine hydrochloride); PSS = poly(styrene sulfonate), EDC = 1-ethyl-3-(3-dimethylaminopropyl)-carbodiimide; NHS = *N*-hydroxysuccinimide.

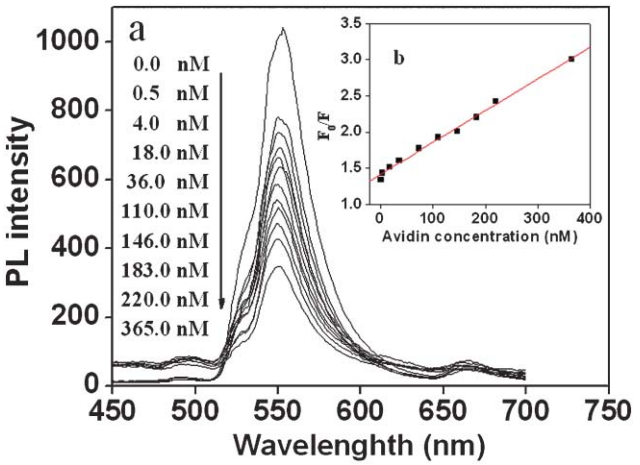

Fig. 17 FRET-based assay of avidin: (a) PL spectra of the FRET system at different concentrations of avidin as indicated (nm); (b) linear relationship between the relative intensity of PL (F_0/F) and the concentration of avidin in the system.

showed the linear relationship between the relative intensity of PL (F_0/F) of the system and the concentration of avidin, where F_0 and F represented the intensity of luminescence in the absence and presence of different amounts of avidin, respectively.

The results indicated that such a FRET system was sensitive and simple for use in biological analyses. By using nonenzymatic glucose modified $LaF_3:Ce^{3+}/Tb^{3+}$ nanocrystals as energy donor and the 3-aminophenylboronic acid modified rhodamine B isothiocyanate as energy acceptor, a simple and sensitive FRET nonenzymatic sensor for glucose has also been successfully developed. Further studies may pave the way to wider applications of these luminescent nanocrystals in ultrasensitive multicolor detection of nucleic acids and proteins, fluorescence immunoassays, and fluorescence imaging performed *in vitro* and *in vivo*.[65,66]

Summary and perspective

This article summarizes our recent progress on the synthesis, assembly and applications of monodisperse nanocrystals. New synthetic strategies are always the bases for the development of materials science while new and novel properties discovered in monodisperse nanocrystal systems push the whole field forward. So a general understanding on the synthesis, assembly and applications seems important for scientists involved in this field. The scientific and technical potential of these novel nanostructures are certainly bright and there are great research opportunities that will be explored by many chemists, physicists and material scientists around this general area of monodisperse nanocrystals.

Acknowledgements

This work was supported by NSFC (90606006), the Foundation for the Author of National Excellent Doctoral Dissertation of China and the State Key Project of Fundamental Research for Nanoscience and Nanotechnology (2006CBON0300).

References

1 A. P. Alivisatos, *Science*, 1996, **271**, 933.
2 C. C. Chen, A. B. Herhold, C. S. Johnson and A. P. Alivisatos, *Science*, 1997, **276**, 398.
3 X. G. Peng, L. Manna, W. D. Yang, J. Wickham, E. Scher, A. Kadavanich and A. P. Alivisatos, *Nature*, 2000, **404**, 59.
4 Y. N. Xia and P. D. Yang, *Adv. Mater.*, 2003, **15**, 353–389.
5 M. Li, H. Schnablegger and S. Mann, *Nature*, 1999, **402**, 393.
6 E. Rabani, D. R. Reichman, P. L. Geissler and L. E. Brus, *Nature*, 2003, **426**, 271.
7 W. D. Luedtke and U. Landman, *J. Phys. Chem.*, 1996, **100**, 13323.
8 X. F. Duan, Y. Huang, Y. Cui, J. F. Wang and C. M. Lieber, *Nature*, 2001, **409**, 66.
9 Y. H. Gao and Y. Bando, *Nature*, 2002, **415**, 599.
10 Z. H. Zhong, F. Qian, D. L. Wang and C. M. Lieber, *Nano Lett.*, 2003, **3**, 343.
11 T. Kuykendall, P. J. Pauzauskie, Y. F. Zhang, J. Goldberger, D. Sirbuly, J. Denlinger and P. D. Yang, *Nat. Mater.*, 2004, **3**, 524.
12 H. M. Chen, R. S. Liu, H. L. Li and H. C. Zeng, *Angew. Chem., Int. Ed.*, 2006, **45**, 2713.
13 W. Lu, J. Fang, K. L. Stokes and J. Lin, *J. Am. Chem. Soc.*, 2004, **126**, 11798.
14 C. T. Black, C. B. Murray, R. L. Sandstrom and S. H. Sun, *Science*, 2000, **290**, 113.
15 M. P. Pileni, *Langmuir*, 1997, **13**, 3266.
16 C. B. Murray, D. J. Norris and M. G. Bawendi, *J. Am. Chem. Soc.*, 1993, **115**, 8706.
17 Y. Yin and A. P. Alivisatos, *Nature*, 2005, **437**, 664.
18 J. M. Phillips, *MRS Bull.*, 2006, **31**, 44.
19 E. V. Shevchenko, D. V. Talapin, N. A. Kotov, S. O'Brien and C. B. Murray, *Nature*, 2006, **439**, 55.
20 Z. Y. Huo, C. Chen and Y. D. Li, *Chem. Commun.*, 2006, 3522.
21 J. F. Liu and Y. D. Li, Synthesis and Self-Assembly of Luminescent Ln^{3+}-Doped $LaVO_4$ Uniform Nanocrystals, *Adv. Mater.*, 2006, DOI: 10.1002/adma.200600336.
22 W. C. W. Chan and S. Nie, *Science*, 1998, **281**, 2016.
23 M. Bruchez, D. J. Moronne, P. Gin, S. Weiss and A. P. Alivisatos, *Science*, 1998, **281**, 2013.
24 R. Narayanan and M. A. El-Sayed, *Nano Lett.*, 2004, **4**, 1343.
25 K. B. Zhou, X. Wang, X. M. Sun, Q. Peng and Y. D. Li, *J. Catal.*, 2005, **229**, 206.
26 J. T. Zhang, J. F. Liu, Q. Peng, X. Wang and Y. D. Li, *Chem. Mater.*, 2006, **18**, 867.
27 J. F. Liu, X. Wang, Q. Peng and Y. D. Li, *Adv. Mater.*, 2005, **17**, 764.
28 Y. D. Li, Y. T. Qian, H. W. Liao, Y. Ding, L. Yang, C. Y. Xu, F. Q. Li and G. Zhou, *Science*, 1998, **281**, 246.
29 Y. Xie, Y. T. Qian, W. Z. Wang, S. Y. Zhang and Y. H. Zhang, *Science*, 1996, **272**, 1926.
30 X. L. Li, Q. Peng, J. X. Yi, X. Wang and Y. D. Li, *Chem. Eur. J.*, 2006, **12**, 2383.
31 H. Deng, X. L. Li, Q. Peng, X. Wang, J. P. Chen and Y. D. Li, *Angew. Chem., Int. Ed.*, 2005, **44**, 2782.
32 S. F. Si, C. H. Li, X. Wang, D. P. Yu, Q. Peng and Y. D. Li, *Cryst. Growth Des.*, 2005, **2**, 391.
33 Y. Zhang, Q. Peng, X. Wang and Y. D. Li, *Chem. Lett.*, 2004, **33**, 1320.
34 Y. Zhang and Y. D. Li, *J. Phys. Chem. B*, 2004, **108**, 17805.
35 J. Xu, J. P. Ge and Y. D. Li, *J. Phys. Chem. B*, 2006, **110**, 2497.
36 L. Y. Wang, J. Bao, L. Wang, F. Zhang and Y. D. Li, *Chem. Eur. J.*, 2006, **12**, 6341.
37 X. Wang, J. Zhuang, Q. Peng and Y. D. Li, *Nature*, 2005, **437**, 121.
38 J. P. Ge, W. Chen, L. P. Liu and Y. D. Li, *Chem. Eur. J.*, 2006, **12**, 6552.
39 X. Liang, X. Wang, J. Zhuang, Y. T. Cheng, D. S. Wang and Y. D. Li, *Adv. Funct. Mater.*, 2006, **16**, 1805.
40 X. Wang, J. Zhuang, Q. Peng and Y. D. Li, *Langmuir*, 2006, **22**, 7364.
41 J. P. Ge, S. Xu, J. Zhuang, X. Wang, Q. Peng and Y. D. Li, *Inorg. Chem.*, 2006, **45**, 4922.
42 J. P. Ge, S. Xu, L. P. Liu and Y. D. Li, *Chem. Eur. J.*, 2006, **12**, 3672–3677.
43 X. Wang, J. Zhuang, Q. Peng and Y. D. Li, *Inorg. Chem.*, 2006, **45**, 6661–6665.
44 L. Y. Wang and Y. D. Li, *Nano Lett.*, 2006, **6**, 1645–1649.
45 J. F. Liu, Q. H. Yao and Y. D. Li, *Appl. Phys. Lett.*, 2006, **88**, 173119.
46 X. Liang, X. Wang, J. Zhuang, Q. Peng and Y. D. Li, Synthesis of $NaYF_4$ Nanocrystals with Predictable Phase and Shape, *Adv. Funct. Mater.*, 2006, DOI: 10.1002/adfm.200600807.
47 X. Wang, J. Zhuang, Q. Peng and Y. D. Li, *Adv. Mater.*, 2006, **18**, 2031–2034.
48 L. Y. Wang and Y. D. Li, *Chem. Mater.*, 2007, **19**, 727.
49 J. M. Lehn, *Angew. Chem., Int. Ed. Engl.*, 1990, **29**, 304.
50 H. Zeng, J. Li, J. P. Liu, Z. L. Wang and S. H. Sun, *Nature*, 2002, **420**, 395.
51 C. J. Xu, K. M. Xu, H. W. Gu, X. F. Zhong, Z. H. Guo, R. K. Zheng, X. X. Zhang and B. Xu, *J. Am. Chem. Soc.*, 2004, **126**, 3392.
52 A. R. Tao and P. D. Yang, *J. Phys. Chem. B*, 2005, **109**, 15687.
53 J. T. Zhang, X. L. Li, X. M. Sun and Y. D. Li, *J. Phys. Chem. B*, 2005, **109**, 12544.
54 A. T. Bell, *Science*, 2003, **299**, 1668.
55 G. A. Somorjai and M. Yang, *Top. Catal.*, 2003, **24**, 61.
56 G. A. Somorjai, in *Proceedings of the Robert A. Welch Foundation Conferences on Chemical Research*, Houston, Texas, November 9–11, 1981; G. A. Somorjai, The surface science of heterogeneous catalysis, *Heterogeneous Catal.*, 1981, **25**, 83–127.
57 B. M. Choudary, R. S. Mulukutla and K. J. Klabunde, *J. Am. Chem. Soc.*, 2003, **125**, 2020.
58 P. K. Stoimenov, V. Zaikovski and K. J. Klabunde, *J. Am. Chem. Soc.*, 2003, **125**, 12907.
59 K. B. Zhou, R. P. Wang, B. Q. Xu and Y. D. Li, *Nanotechnology*, 2006, **17**, 3939.
60 R. Xu, D. S. Wang, J. T. Zhang and Y. D. Li, *Chem. Asian J.*, 2006, **1**, 888.
61 R. Xu, X. Wang, D. S. Wang, K. B. Zhou and Y. D. Li, *J. Catal.*, 2006, **237**, 426.
62 S. Heer, O. Lehmann, M. Hasse and H. U. Güdel, *Angew. Chem., Int. Ed.*, 2003, **42**, 3179.
63 L. Y. Wang, R. X. Yan, Z. Y. Huo, L. Wang, J. H. Zeng, J. Bao, X. Wang, Q. Peng and Y. D. Li, *Angew. Chem., Int. Ed.*, 2005, **44**, 6054–6057.
64 D. Wang, A. L. Rogach and F. Caruso, *Nano Lett.*, 2002, **2**, 857.
65 L. Y. Wang and Y. D. Li, Luminescent Nanocrystal for Nonenzymatic Glucose Determination, *Chem. Eur. J.*, 2007, DOI: 10.1002/chem.200700005.
66 L. Y. Wang and Y. D. Li, *Chem. Commun.*, 2006, 2557–2559.

